Available online at www.sciencedirect.com

ScienceDirect

Ceramics International 40 (2014) 975–983

CERAMICS INTERNATIONAL

www.elsevier.com/locate/ceramint

Physical and chemical properties of multifunctional ZnO nanostructures prepared by precipitation and hydrothermal methods

Sumetha Suwanboon[a,e,*], Pongsaton Amornpitoksuk[b,e], Phuwadol Bangrak[c], Chamnan Randorn[d]

[a]Department of Materials Science and Technology, Faculty of Science, Prince of Songkla University, Hat Yai, Songkhla 90112, Thailand
[b]Department of Chemistry and Center of Excellence for Innovation in Chemistry, Faculty of Science, Prince of Songkla University, Hat Yai, Songkhla 90112, Thailand
[c]School of Science, Walailak University, Nakhon Si Thammarat 80161, Thailand
[d]Department of Chemistry, Faculty of Science, Chiang Mai University, Chiang Mai 50200, Thailand
[e]Center of Excellence in Nanotechnology for Energy (CENE), Prince of Songkla University, Hat Yai, Songkhla 90112, Thailand

Received 16 May 2013; received in revised form 22 June 2013; accepted 24 June 2013
Available online 29 June 2013

Abstract

Spherical, cabbage-like and flower-like ZnO powders were prepared by precipitation and hydrothermal methods. $Zn(CH_3COO)_2 \cdot 2H_2O$, KOH, distilled H_2O and C_3H_9N were used as the zinc source, precipitating agent, solvent and capping agent, respectively. The ZnO powders were characterized by TGA, FTIR, XRD and SEM. The particle shape of the ZnO powders altered when the solution was modified by n-propylamine. The photocatalytic activity of the ZnO powders depended on the particle shape whilst the bactericidal property of the ZnO powders was influenced by both particle shape and defect concentration.

Keywords: A. Powders: chemical preparation; B. Defects; D. ZnO; E. Functional application

1. Introduction

Zinc oxide (ZnO) is a wide band gap (3.37 eV) II–VI compound semiconductor that has received much attention over the past few years because ZnO has a wide range of useful properties including electrical [1], optical [1,2], chemical [2] and magnetic properties [3]. Therefore, ZnO has become extraordinarily important as it can be applied in many applications such as a catalyst [2], for gas sensing [4], for semiconductors [5], for piezoelectric devices [6], UV-shielding materials [7] and an antibacterial agent [8]. As it is such a multifunctional material, research on ZnO powders has focused on their preparation using various methods including a solid state reaction [2], flame spray pyrolysis [9], a microwave-assisted method [10], a sonochemical route [11], sol–gel [12], hydrothermal [4] and precipitation [2] methods. Each method has different advantages and disadvantages, however, the selected method should produce and reproduce the required powders for mass production. Moreover, the cost of the apparatus and equipment should be inexpensive to reduce the production cost when it was to be used in the industry. In this study, the precipitation and hydrothermal methods were chosen to examine the effects of the morphology of the powders on their properties as the morphology can be controlled by these synthetic conditions and the preparation of the powders can be easily scaled-up. Taking into account the various parameters concerned, the n-propylamine concentration that acted as a capping agent was a major factor to influence the morphological changes. Therefore, the effects of the n-propylamine concentration on the characteristics of the ZnO powders prepared by the precipitation and hydrothermal methods were investigated because there have been a few reports [13–16] that have revealed an influence of propylamine. Hsei [13] prepared spherical ZnO nanoparticles by the precipitation method using a mixture of

*Corresponding author at: Department of Materials Science and Technology, Faculty of Science, Prince of Songkla University, Hat Yai, Songkhla 90112, Thailand. Tel.: +66 74 28 82 50; fax: +66 74 21 83 95.
E-mail address: ssuwanboon@yahoo.com (S. Suwanboon).

0272-8842/$ - see front matter © 2013 Elsevier Ltd and Techna Group S.r.l. All rights reserved.
http://dx.doi.org/10.1016/j.ceramint.2013.06.094

ethanol and water as a solvent, n-propylamine as a precipitating agent and triethanolamine as a surface active agent or capping agent. They found that larger particles were obtained when the fraction of ethanol to water ratio increased. Verbakel et al. [14] prepared ZnO–polystyrene diodes by using n-propylamine as a ligand for fabricating the thin film. Wahab et al. [15] synthesized the ZnO nanoparticles by refluxing at 65 °C for 6 h. In their experiment, zinc nitrate hexahydrate, together with methanol, n-propylamine and sodium dodecyl sulfate were used as the source of the zinc, as solvent, precipitating agent and capping agent, respectively. The particle size was in a range of 6–7 nm and spherical shapes were obtained. Ramini et al. [16] investigated the influence of n-propylamine on controlling the morphology of the ZnO powders. They used zinc acetate dihydrate, deionized water, sodium hydroxide and tri-n-propylamine as the zinc source, solvent, precipitating agent and capping agent, respectively. The process was continued at 80 °C for 5 h and they found that the particle shape altered as a function of the tri-n-propylamine concentration and the antibacterial activity depended on the particle shape of the ZnO powders.

As far as our review of publications on this subject, we have found no reports on the influence of n-propylamine that acted as a capping agent on the control of ZnO morphology by the precipitation method at 60 °C and the hydrothermal method at 180 °C. In addition, the dependence of the photocatalytic and bactericidal activities on particle shape and defect concentration was investigated in this study.

2. Experimental

The starting materials used in this study were analytical grade and they were used as received. Zinc acetate dihydrate ($Zn(CH_3COO)_2 \cdot 2H_2O$) was from Sigma-Aldrich, Germany. Potassium hydroxide (KOH) was from Emsure, Germany. n-propylamine (C_3H_9N) was from Fluka, Germany. Methylene blue ($C_{16}H_{18}N_3SCl$) was from UNILAB, Australia.

2.1. Precipitation method

The starting precursor solutions were prepared separately. First, the mixtures of 0.125 mol KOH and 0, 0.025, 0.05 and 0.075 mol C_3H_9N were dissolved separately in 100 mL of distilled water at room temperature by magnetic stirring continuously for 15 min. Secondly, the 0.025 mol $Zn(CH_3COO)_2 \cdot 2H_2O$ was dissolved in 100 mL distilled water at room temperature by magnetic stirring continuously for 15 min. In this study, the mole ratio of C_3H_9N to $Zn(CH_3COO)_2 \cdot 2H_2O$ (R) was kept constant at 0, 1, 2 and 3, respectively. Then, the $Zn(CH_3COO)_2 \cdot 2H_2O$ solution was added dropwise into the C_3H_9N-modified KOH solutions and the reaction products were heated at 60 °C for 1 h before filtering, washing with distilled water until the filtrate was neutral and then rinsing with ethanol, drying at room temperature and finally the powders were characterized by various methods.

2.2. Hydrothermal method

The starting precursor solutions were prepared separately. First, the mixtures of 0.125 mol KOH and 0, 0.025, 0.05 and 0.075 mol C_3H_9N were dissolved separately in 100 mL of distilled water at room temperature by continuous magnetic stirring for 15 min. Secondly, the 0.025 mol $Zn(CH_3COO)_2 \cdot 2H_2O$ was dissolved in 100 mL distilled water at room temperature by continuous magnetic stirring for 15 min. In this study, the mole ratio of C_3H_9N to $Zn(CH_3COO)_2 \cdot 2H_2O$ (R) was kept constant at 0, 1, 2 and 3, respectively. Then, the $Zn(CH_3COO)_2 \cdot 2H_2O$ solution was added dropwise into the C_3H_9N-modified KOH solutions and the reaction products were stirred for 15 min and then transferred into the Teflon-lined reactors. The reaction products were heated at 180 °C for 15 h and then naturally cooled to room temperature before filtering, washing with distilled water until the filtrate was neutral and then rinsing with ethanol, drying at room temperature and finally characterizing them using various methods.

2.3. Characterizations

The as-prepared and calcined ZnO powders were characterized in detail using various techniques. Thermogravimetric analyzer (TGA 7, Perkin Elmer) was used to investigate the thermal decomposition of the undesired species of the ZnO powders. An X-ray powder diffractometer (XRD, X'Pert MPD, Philips) was used to identify the phase formation and the crystallinity of the powders. A Fourier Transform Infrared spectrometer (FTIR, Equinox 55, Bruker) was used to observe the impurities adsorbed on the surface of the powders. A scanning electron microscopy (SEM, Quanta 400, FEI) was used to observe the morphology of the powders. A UV–vis spectrophotometer (UV–vis 2450, Shimadzu) was used to measure the diffuse reflectance spectra of the ZnO powders and a UV–vis spectrophotometer (UV–vis, Lambda 25, Perkin Elmer) was used to measure the absorbance of the MB solution. The Brunauer–Emmett–Teller (BET) method (Autosorb 1 MP, Quantachrome) was used to determine the total surface area of the samples.

2.4. Photocatalytic activity

The photocatalytic degradation of the ZnO powders was examined using UV irradiation on an aqueous MB solution at room temperature. Typically, 150 mg of the ZnO powders were dispersed into 150 mL of 1.5×10^{-5} M MB solution in a glass beaker. The mixtures were stirred for 30 min in the dark to equilibrate the adsorption and desorption of MB on the surface of ZnO powders. Then, the mixtures were irradiated using three parallel blacklight fluorescent tubes (15 W). A 3 mL sample of the MB solution was collected every 30 min for 3 h and each MB solution was centrifuged to separate the powders and the absorbance of the MB solution was measured to determine the concentration of the remaining MB.

2.5. Antibacterial activity

The antibacterial activity of the ZnO powders was examined by a broth microdilution method to evaluate the minimum inhibitory concentration (MIC) value. *Staphylococcus aureus* (*S. aureus*) ATCC 25923 and *Escherichia coli* (*E. coli*) ATCC 25922 were used as representative microorganisms for Gram-positive and Gram-negative bacteria, respectively. In order to examine the antibacterial activity, ZnO powders were suspended in sterile distilled water and sonicated for 20 min to yield a stock solution of 50 mg/mL and the samples were diluted using the two-fold serial dilution method starting with 50 and diluting to 0.78 mg/mL. The bacterial suspensions were prepared in normal saline solution (NSS) with an optical density equivalent to the 0.5 McFarland standard, and diluted to 1:20 in NSS to obtain a final concentration of about 5×10^6 CFU/mL. Then triplicate 50 μL samples of each dilution were applied into a sterile 96-well microtiter plate. To each well was added 10 μL of 0.675% (w/v) reasurin solution as an indicator and 30 μL of 3.3 strength Mueller Hinton Broth (3.3 × MHB). Finally, 10 μL of the bacterial suspension (5×10^6 CFU/mL) was applied to achieve a concentration of 5×10^5 CFU/mL. The microtiter plates were prepared in triplicate. After incubation at 37 °C for 20 h, the lowest concentration at which no color change occurred was taken as the MIC value.

3. Results and discussion

3.1. TGA analysis

The thermal behavior of the as-synthesized ZnO powders was characterized by TGA under a nitrogen flux at a temperature of between 50 and 1000 °C and the heating rate of 10 °C/min. The results are shown in Fig. 1. The as-synthesized ZnO powders prepared by the precipitation method showed a weight loss of about 3.3 wt% over the temperature range of 50–640 °C (Fig. 1a). This small weight loss mostly came from the decomposition of the adsorbed n-propylamine on the surface of the ZnO powders that was not released by the washing and rinsing process. Regarding the thermal behavior of the as-synthesized ZnO powders prepared by the hydrothermal method (Fig. 1b), it was evident that the as-synthesized ZnO powders had a weight loss of 0.6 wt% only in the temperature range of 50–600 °C. From the results obtained, it could be summarized that the ZnO powders prepared by the hydrothermal method exhibited a higher quality and purity than the ZnO powders prepared by the precipitation method.

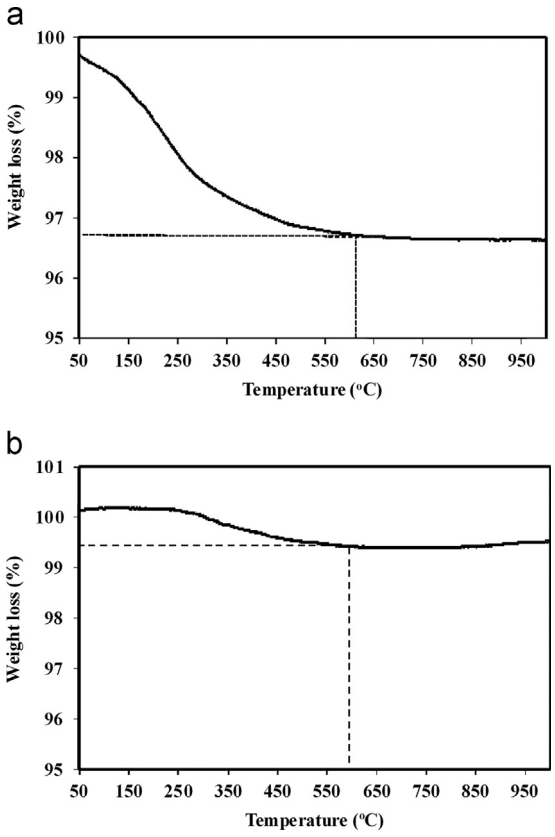

Fig. 1. The thermal analysis of as-synthesized ZnO powders prepared at $R=3$ by different methods (a) precipitation and (b) hydrothermal methods.

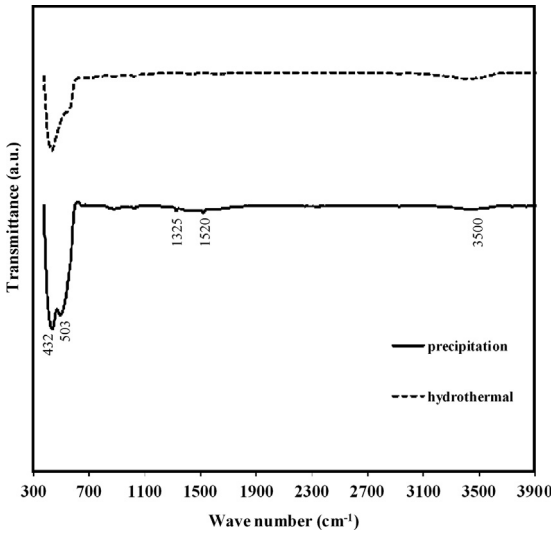

Fig. 2. The FTIR spectra of as-synthesized ZnO powders prepared at $R=3$ by different methods (a) precipitation and (b) hydrothermal methods.

3.2. FTIR analysis

The FTIR spectra of the as-synthesized ZnO powders prepared by using $R=3$ are depicted in Fig. 2.

The FTIR spectra of the ZnO powders prepared by the precipitation and hydrothermal methods showed different absorption peaks. When the precipitation method was used, the as-synthesized ZnO powders showed a broad band centered at about 3500 cm^{-1}, this was attributed to the O–H stretching mode of the hydroxyl group that might come from water adsorbed by the ZnO powders from the humid atmosphere. The absorption peaks at 1520 cm^{-1} and 1325 cm^{-1} were

assigned to a N–H bending mode and a C–N stretching mode of an amine [17], this might be due to a small amount of n-propylamine that had remained on the surface of the ZnO powders. Moreover, the as-synthesized ZnO powders showed two strong absorption peaks at 503 cm^{-1} and 432 cm^{-1}. The absorption peak at 432 cm^{-1} was assigned to the Zn–O stretching mode of ZnO whereas the absorption peak at about 503 cm^{-1} was attributed to the oxygen vacancy in ZnO [18]. When the hydrothermal method was used, the as-synthesized ZnO powders also showed an O–H stretching mode at about 3500 cm^{-1} but the peaks at 1520 cm^{-1} and 1325 cm^{-1} were undetectable. The strong absorption peak at 435 cm^{-1} attributed to the Zn–O stretching mode of ZnO was significant whereas the absorption peak that occurred due to the oxygen vacancy almost vanished. From this point of view, it was concluded that pure ZnO powders were obtained when prepared by the hydrothermal method. The FTIR results corresponded to the TGA obtained. Therefore, the as-synthesized ZnO powders prepared by the precipitation method needed to be calcined before being applied to other investigations. In this study, the ZnO powders were calcined at 600 °C for 1 h in air.

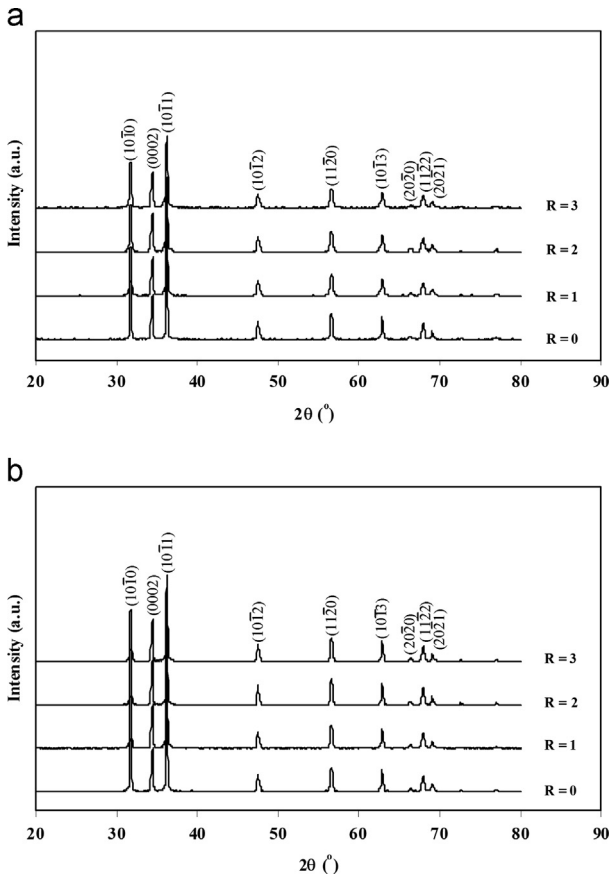

Fig. 3. The XRD patterns of ZnO powders prepared at different n-propylamine concentrations by different methods (a) precipitation and (b) hydrothermal methods.

3.3. XRD analysis

The quality of the ZnO powders prepared from different synthetic methods and n-propylamine concentrations was determined by the XRD technique and are shown in Fig. 3.

It was evident that the calcined ZnO powders prepared by the precipitation method exhibited a hexagonal wurtzite structure without any secondary or impurity phase (Fig. 3a). In a similar way, the as-synthesized ZnO powders prepared by the hydrothermal method also exhibited a hexagonal wurtzite structure without any impurity phase (Fig. 3b).

To investigate the influence of the n-propylamine concentrations on the crystallinity of the ZnO powders, the crystallite size was calculated by the Scherrer's formula [2] (Table 1).

$$D = \frac{k\lambda}{\beta \cos\theta} \quad (1)$$

where D is the crystallite size, k is the shape factor that assumes a value of 0.89 for ZnO, λ is the wavelength of the CuK_α radiation (0.154 nm), β is the full-width at half-maximum of the diffraction peaks and θ is the diffraction angle.

When the precipitation method was used, the crystallite size of the ZnO powders was slightly decreased from 42.65 to 37.52 nm as R was increased from 0 to 2 and when R was further increased to 3, the crystallite size increased again. This might be explained by the influence of the n-propylamine concentration. As we know, ZnO is a polar crystal and crystallizes in the wurzite structure at ambient pressure and temperature. The most common face terminations of the wurtzite ZnO are the polar

Table 1
The physical and antibacterial properties of ZnO powders prepared at different n-propylamine concentrations by different methods.

Methods	R	D (nm)	E_0 (eV)	Minimum inhibitory concentration (mg/mL)	
				S. aureus	*E. coli*
Precipitation	0	42.65	0.09	6.25	–
	1	39.58	0.13	3.125	50
	2	37.52	0.14	3.125	50
	3	39.91	0.15	3.125	50
Hydrothermal	0	41.48	0.06	3.125	50
	1	39.08	0.08	3.125	50
	2	46.91	0.07	0.78	50
	3	47.18	0.06	0.78	50

Zn terminated (0001) and the O terminated ($000\bar{1}$) faces, and non-polar face ($11\bar{2}0$) and ($10\bar{1}0$) faces that both contain an equal number of Zn and O atoms [19]. In this study, the n-propylamine acted as a capping agent due to the nitrogen atom having a lone pair of electrons. Thus, the lone pair of electrons on the nitrogen atom could share with the oxygen atom of ZnO and the adsorption process could progress. As $R \leq 2$, the n-propylamine could adsorb onto the surface of the ZnO nuclei, and then the growth process stopped. When $R = 2$, the adsorption of ZnO nuclei by n-propylamine was the most effective, thus the crystal was the smallest in size. As R was further increased, the n-propylamine might interact with each other, this resulted in a reduction of adsorption efficiency and then the crystal grew [16]. Considering the hydrothermal method, the crystallite size decreased as R was increased from 0 to 1 only. After that, when R was further increased, the crystallite size increased. This could be explained in the same way as for the precipitation method. In addition, the n-propylamine could more easily desorb from the surface of the ZnO nuclei and interact more with each other under the high temperatures and high pressure conditions. Therefore, the crystallite size can grow when $R > 1$. Another reason, is that when the n-propylamine cannot cover the surface of the ZnO nuclei completely, not only can more Zn ions diffuse to the surface of the ZnO nuclei, but also the ZnO nuclei can grow easily by the Ostwald ripening mechanism [20]. These properties assisted the growth process of ZnO in this study.

3.4. Morphological study

In this section, the dependence of the particle shape on the R or n-propylamine concentration and the synthetic route was investigated. When precipitation was used, aggregated spherical particles formed when the ZnO powders were precipitated from the precursor solution without any modification by the n-propylamine as shown in Fig. 4 (at $R = 0$) whereas a cabbage-like structure formed when the precursor solution was modified by n-propylamine (Fig. 4 at $R = 1$–3). The cabbage-like structure was comprised of randomly assembled ZnO nanoplatelets repeatedly as previously observed [21,22]. In this study, the n-propylamine promoted the formation of the nanoplatelet shape might be due to the adsorption of n-propylamine on the ($000\bar{1}$) plane of the ZnO nuclei, resulting in prevention of the growth along the c-axis. Considering the hydrothermal method, the multipods that were composed of small rod-like aggregates as the clusters when R was 0 and 1 as shown in Fig. 5. In addition, when the R was further increased ($R = 2$ and 3), the multipods preferred to grow individually and the aggregation of the multipods was also reduced, to bring about the formation of a flower-like structure (Fig. 5). It was noticeable that each rod of the flower-like structure grew when the R was increased and this was in agreement with the crystallinity obtained from the XRD results. There was a difference between size measurement by XRD and SEM.

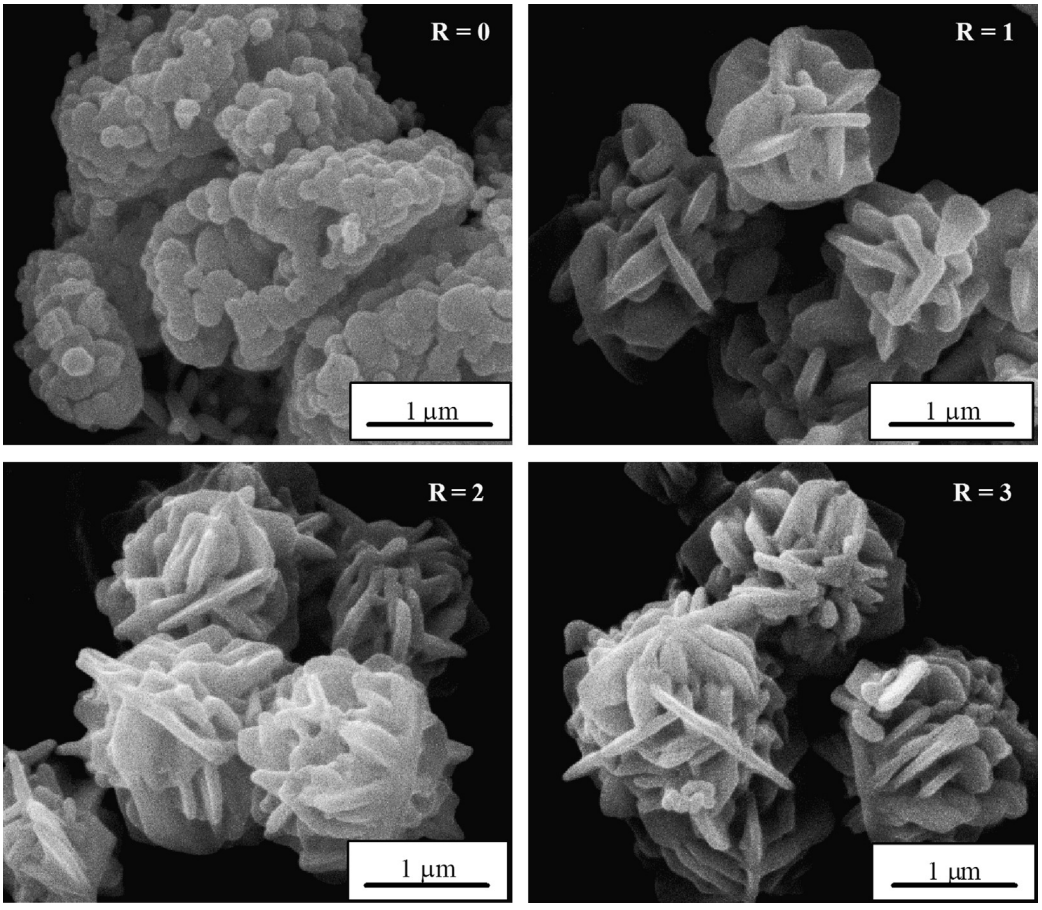

Fig. 4. SEM images of ZnO powders prepared at different n-propylamine concentrations by the precipitation method.

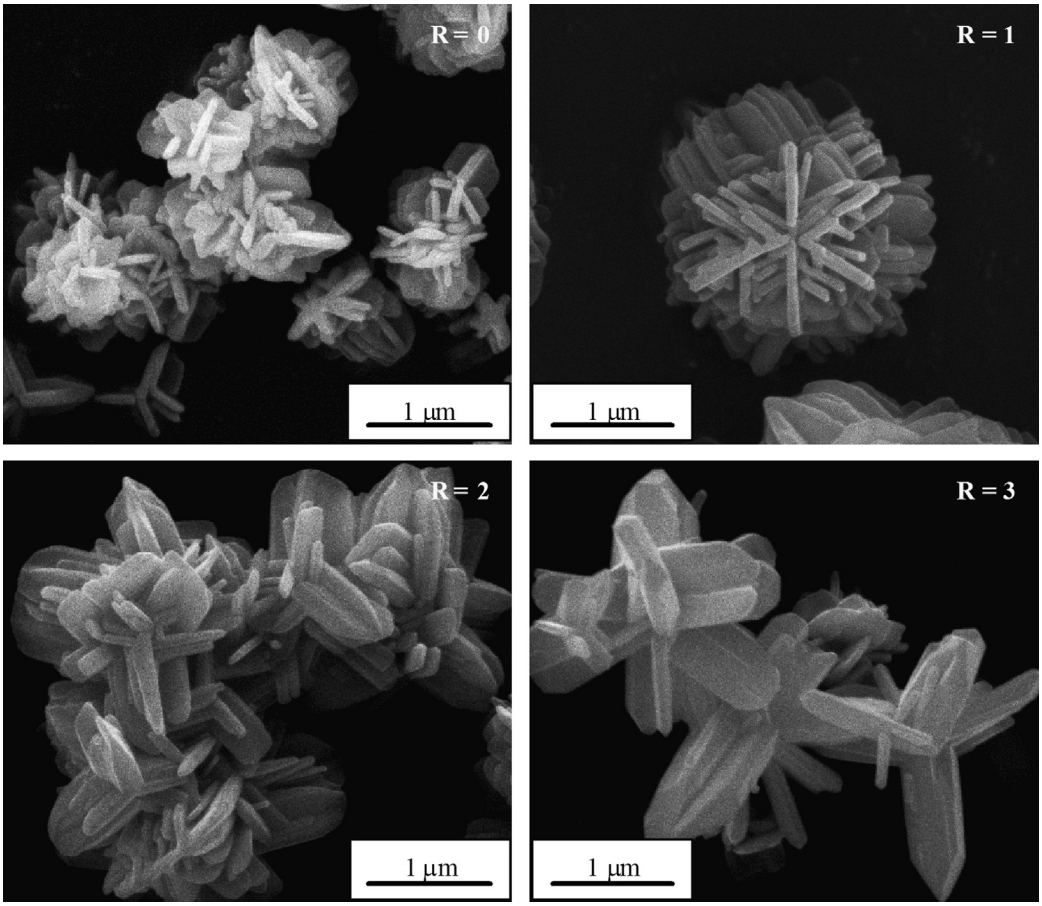

Fig. 5. SEM images of ZnO powders prepared at different n-propylamine concentrations by the hydrothermal method.

In SEM, the particle size was measured by the difference between the visible grain boundaries whereas in the XRD method the measurement was extended to the crystalline region that diffracted X-ray coherently. So, the XRD method was a more stringent criterion and led to smaller size [23].

3.5. Photocatalytic activity

In this study, the photocatalytic activity was investigated by using MB as a dye pollutant. The dependence of the particle shape on the photocatalytic degradation of the MB solution was taken into account. The photocatalytic degradation was estimated from the reduction in absorbance of the MB solution at a maximum wavelength of 664 nm because the MB solution showed the highest intensity at this wavelength. The efficiency of the photocatalytic degradation (*E.P.*) was studied from the following relationship [24]:

$$E.P. = \frac{C}{C_0} = \frac{A}{A_0} \quad (2)$$

where C_0 is the initial concentration of the MB solution, C is the concentration after irradiation at given time intervals, A_0 is the absorbance of the initial MB solution and A is the absorbance of the MB solution after irradiation at the given time intervals.

From Fig. 6, it can be seen that the concentration of MB did not change over the whole range of the irradiation time. Therefore, the self-degradation of MB as a result of UV irradiation was ignored in this study. Considering the photocatalytic efficiency of the ZnO powders prepared by the precipitation method (Fig. 6a), when the suspensions were irradiated for 30 min, the ZnO powders prepared at $R=1$ showed the highest efficiency of photocatalytic degradation of about 82% and the ZnO powders prepared at $R=3$ showed the lowest efficiency of photocatalytic degradation of about 61%, however, the ZnO powders can degrade more than 50% of MB within 30 min. The ZnO powders prepared at $R=0$ and $R=2$ showed a similar efficiency of about 74% and 75%, respectively. Based on the particle shape, the ZnO with a cabbage-like structure that was prepared with different n-propylamine concentrations showed some difference in the size of platelets. As the lower n-propylamine concentration (lower R) was dissolved in the solution, the larger platelets assembled into a cabbage-like structure and the platelets were clearly observed when using $R=1$. Therefore, the ZnO powders prepared at $R=1$ exhibited the highest efficiency for photocatalytic degradation due to it having more specific planes to oxidize the MB molecules [24]. In this study, the total specific surface area of ZnO powders was determined to confirm that the total specific surface area of ZnO is more significant than its surface area. The ZnO powders had the total specific surface area of

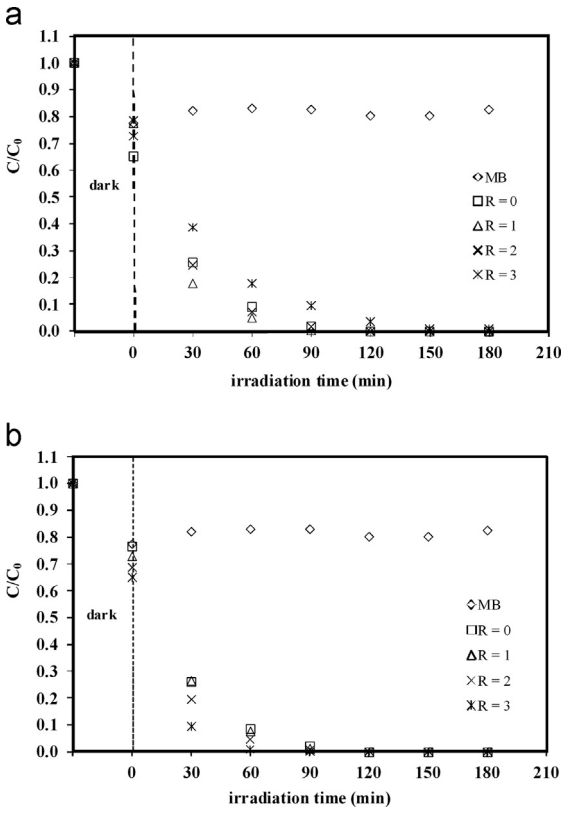

Fig. 6. The photocatalytic efficiency of MB degradation for ZnO powders prepared at different n-propylamine concentrations by different methods (a) precipitation and (b) hydrothermal methods.

3.57, 3.17, 3.62 and 3.74 m^2/g when R was increased from 0 to 3. It was clearly observed that the ZnO powders prepared at $R=1$ had smallest specific surface area, but it exhibited highest photocatalytic efficiency. Therefore, it could be concluded that the specific plane was a key parameter for oxidizing the MB. In this study, the ZnO powders prepared at $R=1$, $R=0$, 2 and $R=3$ completely degraded the MB within 90, 120 and 150 min, respectively.

When the ZnO powders prepared by the hydrothermal method were used as a photocatalyst, the particle shape affected the efficiency of the photocatalytic degradation significantly (Fig. 6b). In this study, the ZnO with the flower-like structure that was composed of larger rods exhibited a better MB degradation compared to the ZnO with the flower-like structures that were composed of smaller rods. Moreover, the flower-like ZnO powders showed higher photocatalytic degradation than the ZnO powders with the aggregated multipod shapes. This can be explained as previously described, the powders with more specific planes exposed to the MB solution degraded the MB better. Moreover, as it is well known, due to the spontaneous polarization of the hexagonal wurtzite structure of ZnO, a divergence in surface energy was produced between the (0001) and (000$\bar{1}$) polar surfaces and the remaining prismatic non-polar surfaces. This energetic divergence actually justified the formation of the observed multipods [25], but it may as well have an influence in the photocatalytic response of the ZnO powders; in fact, for an archetypal photocatalyst like TiO_2 it was accepted that not only the number but also the specific energy of the exposed surface determined the photocatalytic efficiency [26]. When the suspensions were irradiated for 30 min, the ZnO powders showed that the efficiency of photocatalytic degradation was about 90% and 80% when using $R=3$ and $R=2$, respectively whereas the ZnO powders prepared at $R=0$ and $R=1$ showed a similar efficiency of photocatalytic degradation of about 75%. In this case, the ZnO powders can degrade more than 70% of the MB within 30 min, and indicated that the ZnO powders prepared by the hydrothermal method had higher photocatalytic efficiency for degrading MB. The ZnO powders prepared at $R=3$, $R=2$ and R = 0, 1 completely degraded the MB within 60, 90 and 120 min, respectively.

3.6. Bactericidal activity

The MIC values of all ZnO powders against the Gram-positive bacterium *S. aureus* and the Gram-negative bacterium *E. coli* are presented in Table 1. As we know, many factors such as morphology, surface area, surface charge, solubility, degree of aggregation, defect concentration of particle and cell structure of bacteria could influence the damage to the tested bacteria. In this study, the aggregated spherical ZnO particles did not affect the *E. coli* whereas the other ZnO powders had MIC values of 50 mg/mL. Meanwhile, all ZnO powders exhibited a much higher activity towards *S. aureus* than *E. coli*. The difference in the activity of both the bacterias can be explained by the differences in their cell wall structure [8]. As a matter of fact, both Gram-positive bacteria and Gram-negative bacteria have a similar internal structure, but its external structure is different. The external structure of *S. aureus* is composed of a thick peptidoglycan layer that contains teichoic acid and lipiteichoic acid whereas the external structure of *E. coli* is comprised of a thin peptidoglycan layer and a rigid outer membrane that contains lipopolysaccharides and lipoproteins. Generally, the lipopolysaccharides and teichoic acids are used for protection of the cell from antibacterial agents and other hazardous environmental conditions. For this reason, the ZnO powders exhibited less activity towards *E. coli* than *S. aureus* because the *E. coli* has a rigid outer membrane to protect the cell [27]. In addition, the influence of the bactericidal activity from the morphology of the particles and the defect concentration was investigated. The defect concentration such as the oxygen vacancy was estimated from the relationship as follows [28]:

$$\alpha E = \alpha_0 \exp\left(\frac{E}{E_0}\right) \quad (3)$$

where α is the absorption coefficient estimated from the measured absorbance, α_0 is a constant, E is the photon energy and E_0 is an empirical parameter that depends on the defect concentration, temperature and structural disorder. The curves of $\ln(\alpha)$ versus E were plotted as shown in Fig. 7(a) and (b) and the reciprocal of the slopes referred to the defect concentration is presented in Table 1. Reportedly, it is difficult to decide which of the antibacterial mechanism operate in the dark. However, some research workers have proposed that the super-oxide anion

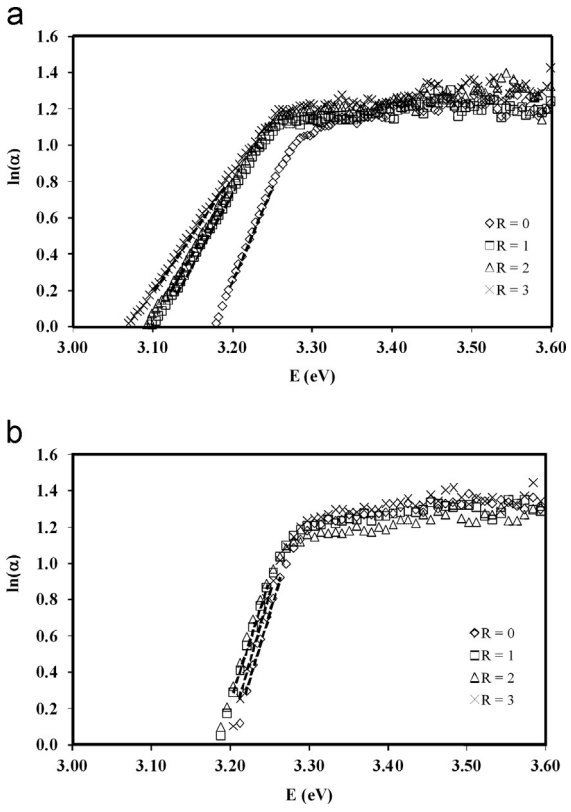

Fig. 7. The plots of ln(α) versus E for evaluating the defect concentration of ZnO powders prepared by different methods (a) precipitation and (b) hydrothermal methods.

radical ($^{\bullet}O_2^-$) is a key factor for inhibiting the bacteria and this was generated from the oxygen dissolved in the solution by single-electron reduction even though UV irradiation was not used [8]. Moreover, Hirota et al. [29] investigated the bactericidal activity in the dark and they confirmed that the super-oxide anion radical ($^{\bullet}O_2^-$) was produced at the surface of samples and the samples that had higher oxygen vacancies produced more super-oxide anion radicals ($^{\bullet}O_2^-$), this resulted in a greater bacterial damage. When the precipitation method was used, ZnO powders prepared at $R=0$ showed the lowest defect concentration or oxygen vacancies whereas the ZnO powders prepared at $R=1$–3 showed higher defect concentrations, thus the ZnO powders prepared at $R=1$–3 can do more damage on the *S. aureus* due to more super-oxide anion radical ($^{\bullet}O_2^-$) being generated as described previously. In addition, the ZnO powders prepared at $R=1$–3 exhibited the cabbage-like structure that assembled from the platelet structure, therefore, the Zn^{2+} ion on the (0001) plane could easily bind to the cell wall of the bacteria [30]. This is another reason that cabbage-like ZnO powders can work against *S. aureus* better than the spherical ZnO powders prepared at $R=0$. Taking into account the ZnO powders prepared by the hydrothermal method, all ZnO powders had a similar defect concentration, so the influence of the super-oxide anion radical ($^{\bullet}O_2^-$) was disregarded. However, the ZnO powders prepared at $R=0$ and 1 as well as $R=2$ and 3 had MIC values of 3.125 and 0.78 mg/mL, respectively. This is because the ZnO powders prepared at $R=0$ and 1 had a similar particle shape, its shapes were different from the ZnO powders prepared at $R=2$ and 3. In this work, the flower-like ZnO powders showed better damage of *S. aureus*. This might be due to the cell wall of the bacteria being more easily bound to the Zn^{2+} ion on the (0001) plane of each platelet ZnO. Moreover, the flower-like ZnO powders prepared at $R=2$ and 3 had more surface abrasiveness caused by the uneven surface textures due to the rough edges and corners that might contribute to the mechanical damage of the cell wall of *S. aureus* [16]. These reasons resulted in better activity against *S. aureus* for ZnO powders prepared at $R=2$ and 3.

4. Conclusions

ZnO powders prepared with a variety of shapes were successfully synthesized by the precipitation method at a temperature of 60 °C for 1 h and the hydrothermal method at a temperature of 180 °C for 15 h. Pure hexagonal ZnO structures were obtained in a single-step synthesis by the hydrothermal method, but the ZnO powders prepared by the precipitation method still contained some adsorbed n-propylamine. However, the pure hexagonal ZnO structure was obtained after calcining at 600 °C in air for 1 h. The spherical shape altered to cabbage-like structure at $R=1$–3 when the precipitation method was used and the assembled multipods structures changed to a flower-like structure at $R=2$–3 when the hydrothermal method was used. When the precipitation method was used, the cabbage-like ZnO powders prepared at $R=1$ exhibited the best photocatalytic degradation of MB and it completely degraded the MB within 90 min. When the hydrothermal process was used, the flower-like ZnO powders prepared at $R=3$ showed the most efficient photocatalytic degradation of MB and it completely degraded the MB within 60 min. The photocatalytic efficiency of the ZnO powders was significantly affected by the particle shape. The particle shape that had more specific planes for MB adsorption that showed the better MB degradation. All ZnO powders can cause more damage to *S. aureus* than to *E. coli* because of the differences in their cell wall structures. The flower-like ZnO powders were most active against *S. aureus* with an MIC value of 0.78 mg/mL due to the powders having more specific planes for contacting the *S. aureus*.

Acknowledgment

The research was supported by the Prince of Songkla University under the Contract number SCI560335S. The authors would like to thank the Center of Excellence for Innovation in Chemistry (PERCH-CIC), Office of the Higher Education Commission, Ministry of Education. CR wishes to thank the National Research University Project under Thailand's Office of the Higher Education Commission. The authors would like to acknowledge Dr. Brian Hodgson for assistance with the English.

References

[1] S.K. Patil, S.S. Shinde, K.Y. Rajpure, Physical properties of spray deposited Ni-doped zinc oxide thin films, Ceramics International 39 (2013) 3901–3907.

[2] S. Suwanboon, P. Amornpitoksuk, A. Sukolrat, N. Muensit, Optical and photocatalytic properties of La-doped ZnO nanoparticles prepared via precipitation and mechanical milling method, Ceramics International 39 (2013) 2811–2819.

[3] S. Yilmaz, J. Nisar, Y. Atasoy, E. McGlynn, R. Ahuja, M. Parlak, E. Bacaksiz, Defect-induced room temperature ferromagnetism in B-doped ZnO, Ceramics International 39 (2013) 4609–4617.

[4] A. Yu, J. Qian, H. Pan, Y. Cui, M. Xu, L. Tu, Q. Chai, X. Zhou, Micro-lotus constructed by Fe-doped ZnO hierarchically porous nanosheets: preparation, characterization and gas sensing property, Sensors and Actuators B: Chemical 158 (2011) 9–16.

[5] C.Y. Zhang, The influence of post-growth annealing on optical and electrical properties of p-type ZnO films, Materials Science in Semiconductor Processing 10 (2007) 215–221.

[6] M. Seo, Y. Jung, D. Lim, D. Cho, Y. Jeong, Piezoelectric and field emitted properties of controlled ZnO nanorods on CNT yarns, Materials Letters 92 (2013) 177–180.

[7] R. Li, S. Yabe, M. Yamashita, S. Momose, S. Yoshida, S. Yin, T. Sato, Synthesis and UV-shielding properties of ZnO- and Cao-doped CeO_2 via soft solution chemical process, Solid State Ionics 151 (2002) 235–241.

[8] N. Talebian, S.M. Amininezhad, M. Doudi, Controllable synthesis ZnO nanoparticles and their morphology-dependent antibacterial and optical properties, Journal of Photochemistry and Photobiology B: Biology 120 (2013) 66–73.

[9] S.D. Lee, S.H. Nam, M.H. Kim, J.H. Boo, Synthesis and photocatalytic property of ZnO nanoparticles prepared by spray pyrolysis method, Physics Procedia 32 (2012) 320–326.

[10] D. Sharma, S. Sharma, B.S. Kaith, J. Rajput, M. Kaur, Synthesis of ZnO nanoparticles using surfacetant free in-air and microwave method, Applied Surface Science 257 (2011) 9661–9672.

[11] I. Kazeminezhad, A. Sadollahkhani, M. Farbod, Synthesis of ZnO nanoparticles and flower-like nanostructures using nonsono- and sono-electrooxidation methods, Materials Letters 92 (2013) 29–32.

[12] M.M. Ba-Abbad, A.A.H. Kadhum, A.B. Mohamad, M.S. Takriff, K. Sopian, The effect of process parameters on the size of ZnO nanoparticles synthesized via the sol–gel technique, Journal of Alloys and Compounds 550 (2013) 63–70.

[13] C.H. Hsieh, Spherical zinc oxide nano particles from zinc acetate in the precipitation method, Journal of the Chinese Chemical Society 54 (2007) 31–34.

[14] F. Verbakel, S.C.J. Meskers, R.A.J. Janssen, Surface modification of zinc oxide nanoparticles influences the electronic memory effects in ZnO-polystyrene diodes, The Journal of Physical Chemistry C Letters 111 (2007) 10150–10153.

[15] R. Wahab, S.K. Tripathy, H.S. Shin, M. Mohapatra, J. Musarrat, A.A. Al-Khedhairy, Photocatalytic oxidation of acetaldehyde with ZnO-quantum dots, Chemical Engineering Journal 226 (2013) 154–160.

[16] M. Ramani, S. Ponnusamy, C. Muthamizhchelvan, From zinc oxide nanoparticles to microflowers: a study of growth kinetics and biocidal activity, Materials Science and Engineering C 32 (2012) 2381–2389.

[17] B. Smith, Infrared Spectral Interpretation, CRC Press, New York, 1999.

[18] G. Xiong, U. Pal, J.G. Serrano, K.B. Ucer, R.T. Williams, Photoluminescence and FTIR study of ZnO nanoparticles: the impurity and defect prespective, Phisica Status Solidi C 3 (2006) 3577–3581.

[19] V.A. Coleman, C. Jagadish, S. Pearton, Zinc oxide bulk, thin film and nanostructures, Elsevier Limited, 2006.

[20] Z. Hu, G. Oskam, P.C. Searson, Influence of solvent on growth of ZnO nanoparticles, Journal of Colliods and Interface Science 263 (2003) 454–460.

[21] P.V. Adhyapak, S.P. Meshram, V. Tomar, D.P. Amalnerkar, I.S. Mulla, Effect of preparation parameters on the morphologically induced photocatalytic activities of hierarchical zinc oxide nanostructures, Ceramics International (2013), http://dx.doi.org/10.1016/j.ceramint.2013.02.076.

[22] F. Li, L. Hu, Z. Li, X. Huang, Influence of temperature on the morphology and luminescence of ZnO micro and nanostructures prepared by CTAB-assisted hydrothermal method, Journal of Alloys and Compounds 465 (2008) L14–L19.

[23] S. Suwanboon, Structural and optical properties of nanocrystalline ZnO powder from sol–gel method, ScienceAsia 34 (2008) 31–34.

[24] H. Usui, Surfactant concentration dependence of structure and photocatalytic properties of zinc oxide rods prepared using chemical synthesis in aqueous solutions, Journal of Colloid and Interface Science 336 (2009) 667–674.

[25] M. Peiteado, T. Jardiel, F. Rubio, A.C. Caballero, Multipod structures of ZnO hydrothermally grown in the presence of Zn_3P_2, Materials Research Bulletin 45 (2010) 1586–1592.

[26] D.G. Calatayud, T. Jardiel, M. Rodíguez, M. Peiteado, D. Fernández-Hevia, A.C. Caballero, Soft solution fluorine-free synthesis of anatase nanoparticles with tailored morphology, Ceramics International 39 (2013) 1195–1202.

[27] S. Suwanboon, P. Amornpitoksuk, P. Bangrak, A. Sukolrat, The dependence of optical properties on the morphology and defects of nanocrystalline ZnO powders and their antibacterial activity, Journal of Ceramic Processing Research 11 (2010) 547–551.

[28] S. Suwanboon, P. Amornpitoksuk, A. Sukolrat, Dependence of optical properties on doping metal, crystallite size and defect concentration of M-doped ZnO nanopowders (M=Al, Mg, Ti), Ceramics International 37 (2011) 1359–1365.

[29] K. Hirota, M. Sugimoto, M. Kato, K. Tsukagoshi, T. Tanigawa, H. Sugimoto, Preparation of zinc oxide ceramics with a sustainable antibacterial activity under dark conditions, Ceramics International 36 (2010) 497–506.

[30] M. Ramani, S. Ponnusamy, C. Muthamizhchelvan, J. Cullen, S. Krishnamurthy, E. Marsili, Morphology-directed synthesis of ZnO nanostructures and their antibacterial activity, Colloids and Surfaces B: Biointerfaces 105 (2013) 24–30.